Responding to Sudden Pollutant Releases in Office Buildings: 1. Framework and Analysis Tools

Michael D. Sohn*, Richard G. Sextro, Ashok J. Gadgil, Joan M. Daisey[1]

Indoor Environment Department

Lawrence Berkeley National Laboratory

One Cyclotron Road

Berkeley, California 94720

* To whom correspondences should be addressed (Mail Stop: 90-3058;

Tel: 510-486-7610; Fax: 510-486-6658; E-mail: mdsohn@lbl.gov)

Accepted for publication in *Indoor Air*

---

[1]Deceased

ABSTRACT

We describe a framework for developing response recommendations to unexpected toxic pollutant releases in commercial buildings. It may be applied in conditions where limited building- and event-specific information is available. The framework is based on a screening-level methodology to develop insights, or rules-of-thumb, into the behavior of airflow and pollutant transport. A three-stage framework is presented: (1) develop a building taxonomy to identify generic, or prototypical, building configurations, (2) characterize uncertainty and conduct simulation modeling to predict typical airflow and pollutant transport behavior, and (3) rank uncertainty contributions to determine how information obtained at a site might reduce uncertainties in the model predictions. The approach is applied to study a hypothetical pollutant release on the first floor of a five-story office building. Key features that affect pollutant transport are identified and described by value-ranges in the building stock. Simulation modeling provides predictions and uncertainty estimates of time-dependent pollutant concentrations, following a release, for a range of indoor and outdoor conditions. In this exercise, we predict concentrations on the fifth floor to be an order of magnitude less than on the first, coefficients of variation greater than 2, and information about the HVAC operation and window position most reducing uncertainty in predicted peak concentrations.

Keywords: uncertainty; decision analysis; simulation; modeling; COMIS; quantile coefficient of variation

PRACTICAL IMPLICATIONS

In the event of a toxic pollutant release in or near a building, first responders are faced with making rapid response decisions with little - and often highly uncertain - information. This paper presents an analytical framework for developing such rapid response decisions and statistical tools for describing and ranking the associated uncertainties. An algorithmic decision tree, based on this analysis framework, can be developed in the future for identifying the best possible rapid response decisions in the field, based on available information. Such software can be placed, for example, on a personal digital assistant (PDA) of first responders.

INTRODUCTION AND MOTIVATION

We present a methodology for developing responses to sudden releases of toxic pollutants in buildings. Developing responses is complicated by several factors: (1) decisions must be made quickly; (2) site- or event-specific information will likely be limited; (3) "incorrect" decisions may result in increased exposure and risk; and (4) first-responders or building operators may be untrained to apply complicated or condition-specific responses. Therefore, it is essential to understand the various parameters that can affect the dispersion of toxic pollutants into and/or within buildings and, in particular, to identify key factors, if they exist, on which response recommendations can be based.

We adopt an approach using a generalized building description and a multizone airflow model - in this case, the COMIS model (Feustel and Rayner-Hooson, 1990; Feustel, 1999) - to explore the factors affecting concentration profiles and resulting occupant exposures for various pollutant release situations. This approach is necessary because a detailed analysis is possible only for a few specific buildings; it is impractical for the entire building stock.

Previous research on fire-safety provided initial guidance for this work. Fire-response protocols are based, in large part, on examining real incidents, but also on computer simulation predictions of smoke behavior in various building configurations and operating conditions. Tamura and Shaw (1976b), Grot and Persily (1986), and Klote and Milke (1992) describe empirical and quantitative methods for estimating smoke transport in large buildings when information about infiltration is limited. They often used an effective leakage area to describe the aggregate effect of numerous poorly defined building leakages. However, their applications focused on the transport of large volumes of smoke during a fire, when the buoyancy-induced flows caused by the fire are so great that they dominate the overall building airflow.

We also drew upon the experience of energy analysts, who use "reference," or prototypical, buildings by specifying only those building characteristics which significantly affect energy consumption, ignoring other building-specific details. For example, to estimate typical energy use in urban settings, Hong et al. (1999) defined a prototypical twelve-story building with only six well-mixed zones on each floor. Others have used reference commercial buildings to estimate baseline energy consumption as a function of building size and service operation (see *e.g.*, NEOS

Corporation, 1993).

Wilson (1988, 1991, 1996) also used computer models of generic houses to compare the protection afforded residents from either sheltering-in-place or evacuation in response to an outdoor airborne pollutant release. His focus was to examine if the building envelop, in general, sufficiently attenuates the impact of the outdoor pollutant plume on predicted adverse health effects. However, he did not consider the effects of alternative building conditions and parameter uncertainties on the results, and hence, has not evaluated how response decisions are affected by these uncertainties.

In an earlier paper (Sohn et al., 1999), we utilized aggregate building descriptions to develop an approach for conducting screening-level airflow and pollutant transport predictions for an office building. In the present paper, we extend that work to specifically quantify the effects of alternative building operating conditions and uncertainties in building parameters. The objectives of this paper are thus to present a framework and the necessary tools for developing generalized response recommendations when faced with limited, or no, event-specific information. The methodology and approach are discussed here; more specific analyses and recommendations will be discussed in a future paper. Recent, related work (Price et al., 2002a,b; LBNL, 2002) has relied - in part - on analyses done for this work.

METHODOLOGY AND APPROACH

We base the framework on a screening-level analysis of dispersion of toxic pollutants indoors. It comprises three stages. First, a taxonomy divides the commercial building stock into four broad building classifications: (1) tall buildings, *e.g.*, offices, (2) flat buildings, *e.g.*, shopping malls, (3) buildings consisting mainly of large atrium-like rooms, *e.g.*, airport terminals and theaters, and (4) buildings with a mixture of large and small rooms and high occupancy, *e.g.*, convention centers. For each building class, we identify the key features affecting airflow, pollutant transport, and exposure, and develop *prototypical* building definitions for each class. Second, we use the prototypical building description and a suitable model to predict airflow and pollutant transport for hypothetical pollutant releases. Third, we quantify the variability in the model predictions using appropriate statistical tools and estimate what site- or event-specific information would reduce prediction uncertainties.

4

To demonstrate this approach, we apply it to a subset of the building taxonomy: intermediate-size commercial buildings. The remainder of this paper describes our analysis of this building class.

Representative Building Taxonomy and Characterization

The prototypical office building comprises those major elements of a typical U.S. commercial office building that can significantly affect airflow and pollutant transport. It is not meant to describe all possible conditions, which would require detailed analysis of site- and event-specific information. Instead, our office building taxonomy is compiled by reviewing the literature (*e.g.*, Tamura and Shaw, 1976b; Turk et al., 1989; Enai et al., 1990; Huang et al., 1991; CEC, 1995; Hong et al., 1999) and conducting various first-order sensitivity analyses to bound the level of detail needed for a screening-level analysis.

Building Configuration

The prototypical intermediate-size commercial office is defined as a five-floor building with an open floorplan (see Figure 1). It consists of: (i) a central interior zone representing office cubicles, conference space, hallways, and general interior building area, (ii) perimeter zones, representing individual window offices, and (iii) a zone, representing elevators, stairs, and utility shafts, that connects adjoining floors via doors. With the exception of the entrance doors on the first floor, each of the five floors are identical. This idealization allows us to study buoyancy-induced pollutant transport in the building, which may not be apparent in single- or two-floor configurations, without incurring the modeling overhead and data needs of a more complex multi-floor building. The total floor area of the prototypical building is 22,000 m^2, which is based on a typical intermediate-sized building in the U.S. Environmental Protection Agency's Building Assessment Survey and Evaluation (BASE) study (USEPA, 2001; Apte et al., 2000). Similar floorplans were also used by Hong et al. (1999) and NEOS Corporation (1993).

In the COMIS model of the building, vertically-stacked well-mixed zones, each with the height equal to the floor height (3.7 m), represent the stairwell and utility shafts. The stacked zones reduce the instantaneous mixing that would be predicted erroneously if a single well-mixed zone was used to represent the entire stairwell. The connection between the stacked zones are represented in the COMIS model using large crack components. Pressure loss between the stacked

zones is insignificant, and much smaller than the buoyancy-induced pressure gradient in the stairwell (see *e.g.*, Klote and Milke, 1992, pg. 56). The model implementation however, is not capable of predicting bi-directional flow between the stacked zones that may occur due to localized temperature gradients. Such complexity, however, is beyond the needs of this work.

HVAC systems vary widely in complexity. For the illustrative application, we selected one common mechanically-driven HVAC system design to limit the range of HVAC conditions considered. Our assumed system supplies air via a single, roof-mounted HVAC fan that can be operated in several modes: 1) no recirculation of return air (*i.e.*, 100% outside air); 2) complete recirculation of return air; 3) an equal mix of return and outdoor air (assumed to be well-mixed by the fan); and 4) the mechanical system turned off. Supplies are fully ducted to each room or space, delivering air at 0.3 m^3/m^2-min uniformly throughout the building (ASHRAE, 1997b). This is equivalent to $\sim$5.5 room air changes per hour in the occupied space. The air returns from each room or space are connected to a common return air plenum servicing the entire building. The supply and return airflow are equal in each zone. The HVAC system is represented in the COMIS model as a well-mixed zone with pressure drops of 500 Pa and 200 Pa in the supply and return duct work, respectively. In addition, we assume there is an outside air damper with leakage characteristics described below.

Uncertainty in Building Model Description

Airflow and pollutant transport predictions depend on values chosen for a number of critical parameters. Table 1 summarizes the model inputs. We base the parameter ranges on the available literature (*e.g.*, Tamura and Shaw, 1976a,b; Klote and Milke, 1992; Grot and Persily, 1986; Persily, 1993; ASHRAE, 1997a; Persily and Ivy, 2001) and use best engineering judgment otherwise. It is important to note that given the limited information, we set wide uncertainty bounds to encompass most - but perhaps not all possible - cases. A description of some of the more critical parameters follows.

Building shell infiltration: There is very limited information about commercial building infiltration/exfiltration in the literature. Databases such as Colliver et al. (1993), ASHRAE (1997a, pg. 29.19), Liddament (1986, ch. 6), and other compilations (Tamura and Shaw, 1976a,b; Klote and Milke, 1992) usually provide only estimates of leakages through

individual components (*e.g.*, electrical sockets, door cracks). Estimating overall wall leakage by summing over the number of individual components is infeasible for this type of analysis. Persily (1993) suggests that the numerous leakage routes are better characterized by aggregating them into whole wall effective leakage areas. His estimated effective leakage areas for tight and very leaky buildings ranged between 0.3 to 5 cm^2/m^2 (@4Pa). We use a uniform uncertainty distribution that spans the entire range.

Perimeter-to-interior-zone air leakage: We assume that much of the air leakage between the perimeter offices and the interior occurs through cracks around individual office doors. Persily (1993) assumes that in residential apartments, the effective leakage area around a door is approximately 75 cm^2 (@4Pa). For comparison, ASHRAE (1997a, pg. 15.3) finds the effective leakage area for pocket doors, the leakiest doors of any reported, to be 14 cm^2 (@4Pa). Acknowledging the large range in values, presumably due in part to characterization and description methods, a wide uniformly distributed range is assumed for each office door (10 cm^2 to 90 cm^2 (@4Pa)). In addition when the HVAC is not operating, interior flows via the HVAC duct system, which are predicted by COMIS, can be significant.

Temperature: Two outside temperature conditions are considered: $30^{\circ}C$ and $10^{\circ}C$. The inside temperature remains at $20^{\circ}C$ at all times and at all locations in the building. COMIS predicts the buoyancy-induced flow caused by the inside/outside temperature difference. We ignore the smaller flows caused by localized temperature differences between zones on a floor, and between floors.

Exterior pressure coefficient ($\mathbf{C}_p$): Wind-induced pressure coefficients are based on estimates presented in the literature (Liddament (1986); Klote and Milke (1992, pg. 28); ASHRAE (1997a, pg. 15.3)). A tail-heavy exponential-uniform distribution is selected to describe the uncertainty in the windward pressure coefficient. Thus, we span the range of pressure coefficients, but with emphasis on higher values in the range, since most of the values reported in the literature were high. For the side and leeward coefficients, we use a uniformly distributed range. A single pressure coefficient is assigned to an entire building wall. The wind is assumed unidirectional into one of the long faces of the building, as illustrated in Figure 1 and a with a range in speed between 1 and 5 m/s, as discussed in Table 1.

HVAC damper leakage: When the HVAC is not operating, we include the possibility of a

faulty shut-off damper that controls fresh air entry into the HVAC system. A partially open

damper can allow the buoyancy-induced flow - caused by the temperature difference

between building interior and exterior - through the HVAC system, a condition commonly

found in real buildings. Employing a log-uniform distribution recognizes that in general the

leakage is small, but allows for the occasional large leak.

Airflow and Pollutant Transport Simulations

We selected the COMIS airflow network model (Feustel and Rayner-Hooson, 1990; Feustel, 1999)

to predict airflow and concentration profiles within the prototypical building. The COMIS model

simulates the pressure distribution within a building based on HVAC system operation and the

interaction of the building with the external environment (wind and air temperature). The air

and contaminant transport into and within the building is driven by this pressure distribution.

All of the air flows are steady-state, as we have not assumed any dynamic changes in the

controlling parameters. Each zone is assumed to be instantaneously well-mixed and the resulting

zonal contaminant concentration profiles vary, depending upon the location of the contaminant

source, the airflow distribution within the building and any air exchange to the outside

(ventilation). Contaminants are assumed to be dilute and well-mixed, so their transport behavior

is the same as the air. For these simulations, we have not incorporated contaminant behavior,

such as deposition to or sorption on surfaces. COMIS has been applied to make predictions, and

the predictions experimentally verified, for airflow and pollutant transport in multi-story low- and

high-rise residences (Feustel et al., 1985; Sextro et al., 1999), small office buildings (Feustel, 1990),

controlled experimental test houses (Haghighat and Megri, 1996), and single-family houses (Zhao

et al., 1998).

The prototypical building representation was used to create 2000 distinct input files for

COMIS simulation. For this purpose, each parameter was randomly sampled from within its

distribution, uncorrelated with the values sampled for other parameters. Thus the 2000 input files

all represented the same floorplan and building layout, but each file had a unique and

uncorrelated combination of values for the parameters displayed in Table 1. The parameter

sampling used a stratified sampling routine (Latin Hypercube in this case). For each input file,

the COMIS simulation predicted the temporal and spatial transport of a contaminant released in the central zone of the first floor. These simulations thus propagated the input parameter variability to model prediction end-points. By examining means and variances of predicted airflows and concentrations at increasing sample sizes, 2000 realizations were found adequate to describe most of the variability in the model predictions, though not at the extreme limits of the probability intervals. Each simulation takes about one minute of CPU time on a Pentium II PC. The 2000 simulations form the basis for further analysis. The results of the simulations are discussed in the Illustrative Results and Discussion section.

Quantifying the Effects of Input Uncertainty

The third stage of the framework examines whether the screening-level analysis can lead to robust decisions given the uncertainties in the modeling parameters. This examination is based on formal decision analysis methods (see *e.g.*, Morgan and Henrion, 1990; Dakins et al., 1996; Dakins, 1999), but simplified to be appropriate for screening-level analysis. Two components are necessary for this examination, a robust uncertainty estimator and a measure of the expected reduction in uncertainty in end-point predictions resulting from incremental information about the event (either in terms of building parameters or release details).

Three uncertainty estimators are considered: the standard deviation, coefficient of variation (CV), and a bounded estimator that we call a quantile coefficient of variation (Equation 1):

$$qCV = \frac{(q_{0.95} - q_{0.05})}{q_{0.50}} \tag{1}$$

where q_i is the ith probability quantile. The standard deviation and coefficient of variation are classical summary statistics based on the full variation between all values of a given model end-point. The qCV is a bounded estimator. It reduces the chance that outlier model simulations - based on possible, but unlikely combinations of model inputs – would overwhelm the uncertainty estimates. By defining the variation component of the qCV (*i.e.*, the numerator) as the width of the two-sided 90% interquantile range, potential outlier model simulations beyond this confidence interval are ignored. Normalization by the median, $q_{0.50}$, serves to more equally weight the relative significance of each of the variances (Morgan and Henrion, 1990, pg. 175). The selection

of a 90% interquantile range is somewhat arbitrary; we selected it as a balance between characterizing much of the variance in the predictions yet excluding some of the extreme values. Alternative confidence bounds and measures with these properties could have been also selected (see *e.g.*, Beyer, 1987, pg. 520).

The expected reduction in uncertainty in a model endpoint is estimated using a simplified value-of-information decision analysis method (Morgan and Henrion, 1990; Dakins et al., 1996; Dakins, 1999). It is based on the expected reduction in end-point uncertainty if uncertainty in any one model parameter was reduced - for example, by 90% if site-specific information is obtained. The *a priori* reduction in uncertainty is an *expectation* and cannot be precisely estimated before the site-specific information is obtained. This is because the numerical value of the model parameter can fall anywhere in the full range. Thus, to estimate the expected reduction in uncertainty for a given model input parameter, the analysis is executed as follows:

1. Divide the uncertainty range into equally spaced probability bins. For example, parsing into ten bins yields bins of width 10% (*i.e.*, 0-10%, 10%-20%, 20%-30% etc.). The median of each bin represents a possible value of the parameter. The width of the bin represents the uncertainty in the parameter value after obtaining information. In other words, the information gathered by the first-responder still results in uncertainty in the estimation of the model parameter.

2. Parse the model simulations (we used 2000 as discussed in the previous section) into the bins according to the parameter value used in the simulation. This yields about 200 simulations per bin for the ten-bin example.

3. For simulations in each bin, predict model end-points of interest (*e.g.*, the peak concentration in a room) and estimate the uncertainty, U_i, using the robust estimators discussed above; where i represents the bin number, *i.e.*, 1 through 10 for the ten-bin example.

4. The expected uncertainty in the model predictions after uncertainty in the model input parameter is reduced is the average of the uncertainty estimates: $E[U] = \frac{1}{n} \sum_i^n U_i$; where n is the number of bins. The expected reduction after information is obtained is the difference

10

between this estimate and the uncertainty averaged over all 2000 simulations (*i.e.*, before information is obtained).

The process can be repeated for each uncertain model input by re-parsing the 2000 model simulations. For uncertainty in the HVAC status, window position, and the outside temperature, the bins are divided into the discrete conditions rather than the ten bins used for the continuous model parameters. We did not consider the possibility of error in gathering information about the discrete parameters since there is such great aggregation of prediction variabilities already in each of their values.

ILLUSTRATIVE RESULTS AND DISCUSSION

Figure 2 illustrates the median and range of predicted airflows between the floors via the stairwell. The wide span between the two-sided 90% confidence interval illustrates the extent to which the variability in the model inputs affects uncertainty in the the airflow predictions. The figure also illustrates how a single model parameter can have dramatic effects on the predicted airflow. For example, buoyancy forces can drive the flow up the stairwell when $T_{outside} < T_{inside}$ (Figure 2a) or in the opposite direction when $T_{outside} > T_{inside}$ (Figure 2b), irrespective of the HVAC operation.

Figure 3 presents the predicted pollutant concentration profiles in the central zone of the first and fifth floors for a 1 kg contaminant release lasting 1000 seconds (16 min. 40 sec.), at a release rate of 1 g/s. The release rate and duration are not critical since the concentration predictions are linear, and permit normalization and superposition. The wide uncertainty bounds (coefficients of variation typically greater than 2) result from the wide variability in the model inputs. The concentrations on the fifth floor remain lower by at least an order of magnitude than those on the first floor. The concentrations in perimeter zones, though not illustrated here, are approximately 30% lower than those in the central zone on the same floor, but with similar time-series profiles. The spatial concentration differences between zones and floors of the building describe the extent to which a gaseous pollutant mixes and transports within the building. These rules-of-thumb generalizations will help first-responders and exposure assessment analysts understand the level of airborne concentrations, and ultimately exposures, that may result from a pollutant release. For example, without any response intervention or knowing any additional event-specific information,

11

first-responders should expect, in this example, at least an order of magnitude attenuation in concentration between the top and bottom floors for a release on the first floor of a five-floor building. Though not shown, the concentrations are predicted to be even lower on the intervening floors than on the fifth floor.

Figure 3 also illustrates the time delay for the first-floor release to reach the fifth floor. For example, the median concentration predictions (denoted by the solid lines in Figure 3) show the concentration on the fifth floor peaking only one minute later than the peak on the first floor. At the 95% quantile, however, the fifth floor concentration peaks as much as 15 minutes after peaking on the first floor. Hence the pollutant will, in most cases, quickly transport through the building but with the possibility, in rarer cases, of transporting much more slowly.

These rules-of-thumb generalizations are not without difficulties. They are greatly affected by the input uncertainties, evidenced by the wide uncertainty bounds in Figures 2 and 3. Moreover, changes in just one input parameter can dramatically alter the concentration predictions. To illustrate, Figure 4 shows the cumulative distribution function[2] (CDF) at t=16.7 minutes (*i.e.*, at the end of the contaminant release) for the central zone of the first and fifth floors for various HVAC operations. The CDF for the first floor concentrations (Figure 4a), shows much greater predicted concentrations and with more uncertainty (denoted by the low slope of the CDF line) for HVAC not operating, than when the HVAC system operates. The amount of recirculation has a negligible effect on the CDF. Predictions for the fifth floor, on the other hand, show the concentrations varying greatly by the amount of air recirculation in the HVAC system (Figure 4b). For example, the predicted concentrations between the HVAC operating at full recirculation and that at 50% recirculation differ by more than 100%.

To demonstrate the third stage of our framework, we compare the ranking of the value of information for a given model end-point prediction. Figure 5 shows such a comparison using first and fifth floor predictions of the peak concentration as the end-point. It summarizes the expected uncertainty reduction resulting from additional information about each of the model inputs. Ninety percent uncertainty reductions about the parameter were assumed and ten probability bins were used in this demonstration.

---

[2] A CDF plot summarizes the range of model predictions found in the simulations according to probability quantiles. For example, the concentration at a CDF value of 0.5 is the median.

For the uncertainty reductions in first floor predictions (first column of Figure 5), the standard deviation and CV estimates both rank information about the window position, to some degree, more important than that about the HVAC operation. The qCV, however, ranks the information about HVAC operation more important. Though the differences are subtle, we expect that reducing the effects of extreme model results in the qCV estimates improves our description of the general model prediction uncertainties, particularly since generic response recommendations will be based more on general trends than on extreme cases. Uncertainty reduction estimates for fifth floor peak concentrations (second column of plots in Figure 5) are consistent with those for the first floor except for the HVAC operation using the CV and qCV estimators. First, the CV does not predict the HVAC operation to be an important contributor to the uncertainty. This is because even within a given HVAC operating condition, the normalized uncertainty of the CV is still very high. Second, the expected reductions using the qCV estimator are not predicted because the denominator in Equation 1, the median, is predicted to be zero when the HVAC is operating with no recirculation. This should not preclude using a qCV estimator with the median as the normalizing factor, since only in rare cases is there a non-zero interquantile range and a zero concentration median.

In summary, information about (1) window and door positions, and (2) the HVAC operation, would most reduce uncertainty in the predictions according to all of the three uncertainty characterization methods. One might suspect that this is because both are averaged over only a few intervals (four HVAC operating conditions, or three window positions) while parameters with continuous uncertainty distributions are averaged over ten intervals. However, the outside temperature uncertainty is averaged over only two intervals, yet is not a significant contributor to the end-point uncertainty.

SUMMARY AND CONCLUSIONS

In the event of a toxic pollutant release in or near a building, first responders are faced with making rapid response decisions with little - and often highly uncertain - information. We present a three-stage framework for formulating and assessing response recommendations given uncertainties in both the "input knowledge" and the possible outcomes. This approach is based on a screening level methodology, thus simplifying the extremely detailed (and sometimes infeasible)

analysis required by rigorous decision analysis approaches. Combining the building-specific input into a few aggregated input parameters for the airflow modeling, with uncertainty distributions describing variability in the building stock, simplifies the model computations and statistical analyses. Moreover, it improves the ability of analysts to (i) describe uncertainty ranges in the inputs from literature and best-engineering estimates, and (ii) identify the critical inputs for specific model end-point predictions. It also lays the foundation for future analyses designed to provide actual response recommendations for minimizing potential adverse health effects.

This analysis is developed around a building taxonomy which we illustrate with a prototypical intermediate-sized commercial building. To describe pollutant dispersion within the prototypical building, we develop a set of model input parameter distributions - but only parameters likely to have significant influence on the airflow and pollutant transport are assigned uncertainty bounds.

The simulation modeling propagates input uncertainty into uncertainties in the resulting model predictions. Model predictions identify the ranges of typical airflows and allow us to examine how much influence each individual model parameter can have on the model predictions. The pollutant transport predictions for a first floor release produce typical spatial and temporal concentration profiles, and show how lack of building-specific information can result in extremely wide output uncertainty bounds. Summary descriptions, such as the order of magnitude concentration attenuation between the first and fifth floors, and the greater than a factor of two range in the coefficients of variation, are the types of generalized information that will assist decision makers in developing generic plans and responses.

The important results from this analytical approach are a set of tools for (i) describing uncertainty in the model predictions and (ii) ranking model input parameters according to their impact on the expected reduction in model prediction uncertainties. The normalized interquantile range estimator (qCV) is a useful tool for estimating screening-level uncertainty. It limits the extent to which extreme and outlier model predictions can dominate uncertainty estimates and it offers an even weighting of the relative importance of each of the variances in the model predictions. This can be important, for example, when wide uncertainty in model inputs results in parameter combinations and model predictions that are feasible but highly unlikely. However, in our illustration, we found only subtle differences between the estimators. More testing will be needed to measure the robustness of the qCV for this task.

Ranking the effects of each model input provides us with a quick and programmable algorithm for determining, in an actual response situation, what information will most reduce the uncertainty in the end-point predictions. In the illustrative application, knowledge about the window and door positions, and the HVAC operation status yields the greatest reductions in uncertainty for predictions of the peak concentration on the first-floor. On the other hand, for fifth floor predictions, information about the HVAC system status does not reduce uncertainty substantially.

In the future, we plan to use these tools to develop response recommendations for minimizing adverse health effects based on exposure and risk modeling (see *e.g.*, Price et al., 2002b,a; LBNL, 2002). The analysis will require integrating the airflow and pollutant transport predictions with exposure and risk modeling to estimate how variability and uncertainty at each stage of the analysis contributes to uncertainty in the overall decision-making.

References

Apte M.G., Fisk W.J. and Daisey J.M. (2000) "Association between indoor CO2 concentrations and sick building syndrome symptoms in US office buildings: An analysis of the 1994-1996 BASE study data", *Indoor Air*, **10**, 246–257.

ASHRAE (1997a) *Handbook of Fundamentals*, American Society of Heating, Refrigerating and Air Conditioning Engeering, Atlanta, GA.

ASHRAE (1997b) *Pocket Guide for Air Conditioning, Heating, Ventilation, Refrigration,* American Society of Heating, Refrigerating and Air Conditioning Engeering, Atlanta, GA.

Beyer W.H., ed. (1987) *CRC Standard Mathematical Tables*, 28th edition, CRC Press, Boca Raton, FL.

CEC (1995) *Air Change Rates in Non-residential Buildings in California, Report P400-91-034BCN*, California Energy Commission, Sacramento.

Colliver D.G., Murphy W.E. and Sun W. (1993) *Development of a Building Component Air Leakage Database, Report RP-438*, ASHRAE, University of Kentucky, Lexington.

Dakins M.E. (1999) "The value of the value of information", *Human and Ecological Risk Assessment*, **5**, 281–289.

Dakins M.E., Toll J.E., Small M.J. and Brand K.P. (1996) "Risk-based environmental remediation: Bayesian Monte Carlo analysis and the expected value of sample information", *Risk Analysis*, **16**, 67–79.

Enai M., Shaw C., Reardon J. and Magee R. (1990) "Multiple tracer gas techniques for measuring interzonal airflows for three interconnected spaces", *ASHRAE Transactions*, **1**, 590–598.

Feustel H.E. (1990) "Measurements of air permeability in multizone buildings", *Energy and Buildings*, **14**, 103–116.

Feustel H.E. (1999) "COMIS - An international multizone air-flow and contaminant transport model", *Energy and Buildings*, **30**, 3–18.

Feustel H.E. and Rayner-Hooson A. (1990) *COMIS Fundamentals. LBL-28560*, Lawrence Berkeley National Laboratory, California.

Feustel H.E., Zuercher C.H., Diamond R., Dickinson B., Grimsrud D. and Lipschutz R. (1985) "Temperature- and wind-induced air flow patterns in a staircase. Computer modelling and experimental verification", *Energy and Buildings*, **8**, 105–122.

Grot R.A. and Persily A.K. (1986) "Measured air infiltration and ventilation rates in eight large office buildings", in H.R. Trechsel and P.L. Lagus, eds., "Measured Air Leakage of Buildings. ASTM STP 904", American Society of Testing and Materials.

Haghighat F. and Megri A.C. (1996) "A comprehensive validation of two airflow models - COMIS and CONTAM", *Indoor Air*, **6**, 278–288.

Hong T., Chou S.K. and Bong T.Y. (1999) "A design day for building load and energy estimation", *Building and Environment*, **34**, 469–477.

Huang J., Akbari H., Rainer L. and Ritschard R. (1991) *Prototypical Commercial Buildings for 20 Urban Market Areas. LBL-29798*, Lawrence Berkeley National Laboratory, California.

Klote J.H. and Milke J.A. (1992) *Design of Smoke Management Systems*, ASHRAE, Atlanta, GA.

LBNL (2002) *http://securebuildings.lbl.gov/*.

Liddament M.W. (1986) *Air Infiltration Calculation Techniques - An Application Guide. AIVC Document: AIC-AG-1-86*, AIVC, United Kingdom.

Morgan M.G. and Henrion M. (1990) *Uncertainty, A Guide to Dealing with Uncertainty in Quantitative Risk and Policy Analysis*, Cambridge University Press, United Kingdom.

NEOS Corporation (1993) *Technology Energy Saving: Summary of Building Prototype Descriptions and Detailed Measure Tables*, Sacramento, California.

Persily A.K. (1993) "Modeling radon transport in multistory residential buildings", in N.L. Nagda, ed., "Modeling of Indoor Air Quality and Exposure, ASTM STP 1205", American Society of Testing and Materials, Philadelphia, PA.

Persily A.K. and Ivy E.M. (2001) *Input Data for Multizone Airflow and IAQ Analysis NISTIR 6585*, National Institute of Standards and Technology, Gaithersburg, MD.

Price P.N., Delp W., Sohn M.D., Thatcher T.L., Lorenzetti D.M., Sextro R.G., Gadgil A.G., Derby E. and Jarvis S. (2002a) *Advice for first responders to a building during a chemical or biological attack. LBNL/PUB-867*, Lawrence Berekeley National Laboratory, California.

Price P.N., Lorenzetti D.M., Gadgil A.J., Sohn M.D., Delp W. and Jarvis S. (2002b) *Information for first responders to a chemical or biological attack. LBNL/PUB-866*, Lawrence Berkeley National Laboratory, California.

Sextro R.G., Daisey J.M., Feustel H.E., Dickerhoff D.J. and Jump C. (1999) "Comparison of modeled and measured tracer gas concentrations in a multizone building", in "Proceedings 8th Int. Conf. on Indoor Air Quality & Climate, Indoor Air 1999", Paper No. 1-696.

Sohn M.D., Daisey J.M. and Feustel H.E. (1999) "Characterizing indoor airflow and pollutant transport using simulation modeling for prototypical buildings. 1. Office buildings", in "Proceedings 8th Int. Conf. on Indoor Air Quality & Climate, Indoor Air 1999", Paper No. 4-719.

Tamura G.T. and Shaw C.Y. (1976a) "Air leakage data for the design of elevator and stair shaft pressurization systems", *ASHRAE Transactions*, **82**, 179–190.

Tamura G.T. and Shaw C.Y. (1976b) "Studies on exterior wall air tightness and air infiltration of tall buildings", *ASHRAE Transactions*, **82**, 122–134.

Turk B.H., Grimsrud D.T., Brown J.T., Geisling-Sobotka K.L., Harrison J. and Prill R.J. (1989) "Commercial building ventilation rates and particle concentrations", *ASHRAE Transactions*, **95**, 422–433.

USEPA (2001) *Building Assessment Survey and Evaluation (BASE) study.* *http* : *//www.epa.gov/iaq/largebldgs/base_page.htm.*

Wilson D.J. (1988) "Variation of indoor shelter effectiveness caused by air leakage variablility of houses in Canada and the USA", in "Proceedings U.S. EPA/FEMA Conference on the Effective Use of In-Place Sheltering as a Potential Option to Evacuation During Chemical Release Emergencies", Emmitsburg, MD.

Wilson D.J. (1991) "Effectiveness of indoor sheltering during long duration toxic gas release", in "Proceedings ER'91 Emergency Response Conference on Technological Response to Dangerous Substances Accidents", Calgary, Alberta.

Wilson D.J. (1996) "Do leaky buildings provide effective shelter?", in "Proceedings 10th Annual Conference Major Industrial Accidents Council of Canada", Edmonton, Alberta.

Zhao Y., Yoshino H. and Okuyama H. (1998) "Evaluation of the COMIS model by comparing simulation and measurement of airflow and pollutant concentration", *Indoor Air*, **8**, 123–130.

Table 1: Building and meteorological uncertainties. The third column, labeled "Distribution" refers to the probability density function describing the uncertainty.

Parameter	Range	Distribution
Wind Speed	1 to 5 m/s	uniform
Pressure Coefficient $(C_p)^1$	windward: 0.2 to 0.9	exponential-uniform
	sides: -0.5 to -0.9	uniform
	leeward: -0.2 to -0.6	uniform
Building Shell Infiltration	0.3 to 5 cm^2/m^2 @4Pa	uniform
Perimeter-to-Interior-Zone Leakage	10 to 90 cm^2 @4Pa, per office	uniform
Combined Elevator & Stairwell Door Leakage	190 to 390 cm^2 @4Pa	uniform
HVAC Damper Leakage	0 to 2000 cm^2 @4Pa	log-uniform
Door & Window Position^2	i) all open	equiprobable
	ii) all closed	
	iii) all exterior doors & windows closed, all interior doors open	
HVAC Status	i) off	equiprobable
	ii) on, full recirculation	
	iii) on, 50% recirculation	
	iv) on, no recirculation	
Temperature	i) outside: 30^oC; inside: 20^oC	equiprobable
	ii) outside: 10^oC; inside: 20^oC	

^{1} Wind direction is shown in Figure 1.

^{2} Size of each window and door is 2 m^2 and 2.5 m^2, respectively.

(a)

interior open–
plan offices

Wind

80m

perimeter
closed offices

stairwell

55m

(b)

stairwell

3.7 m

interior open–
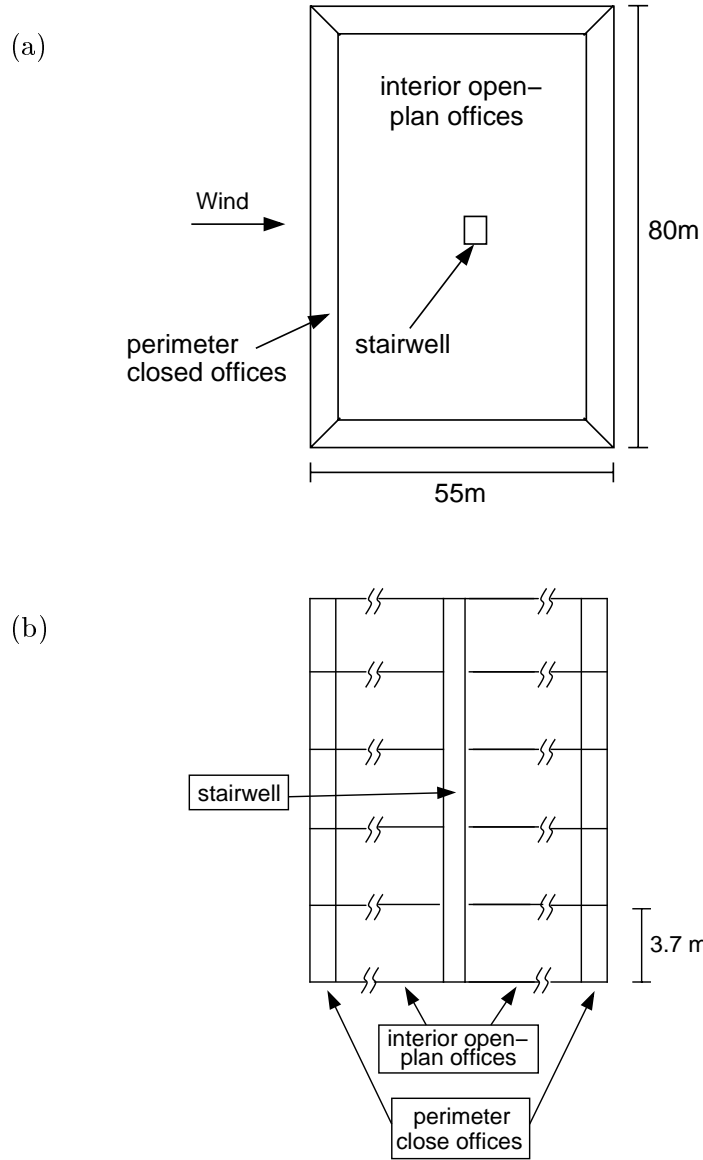plan offices

perimeter
close offices

Figure 1: Illustration of the (a) plan and (b) cross-sectional views of the prototypical open-style commercial building. The floorplan is identical on each floor. The first floor has doors and hallway on the upwind-side of the building connecting the outside with the interior open-plan offices. Based on five-meter square offices, the long- and short-side perimeter zones represent fifteen and ten offices, respectively. The height of each floor includes any plenum area above the occupied space. Each office is connected to the interior space by a closable door.
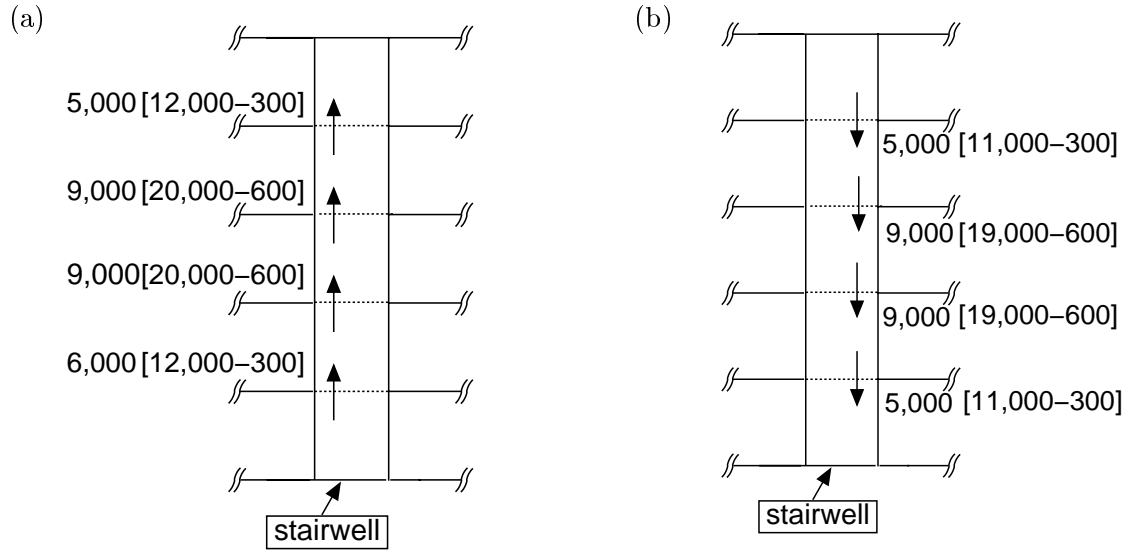
Figure 2: Airflow in the stairwell (m^3/hr). The values indicate the median and 90% confidence interval when (a) $T_{outside} < T_{inside}$ and (b) $T_{outside} > T_{inside}$.

(a)

(b)

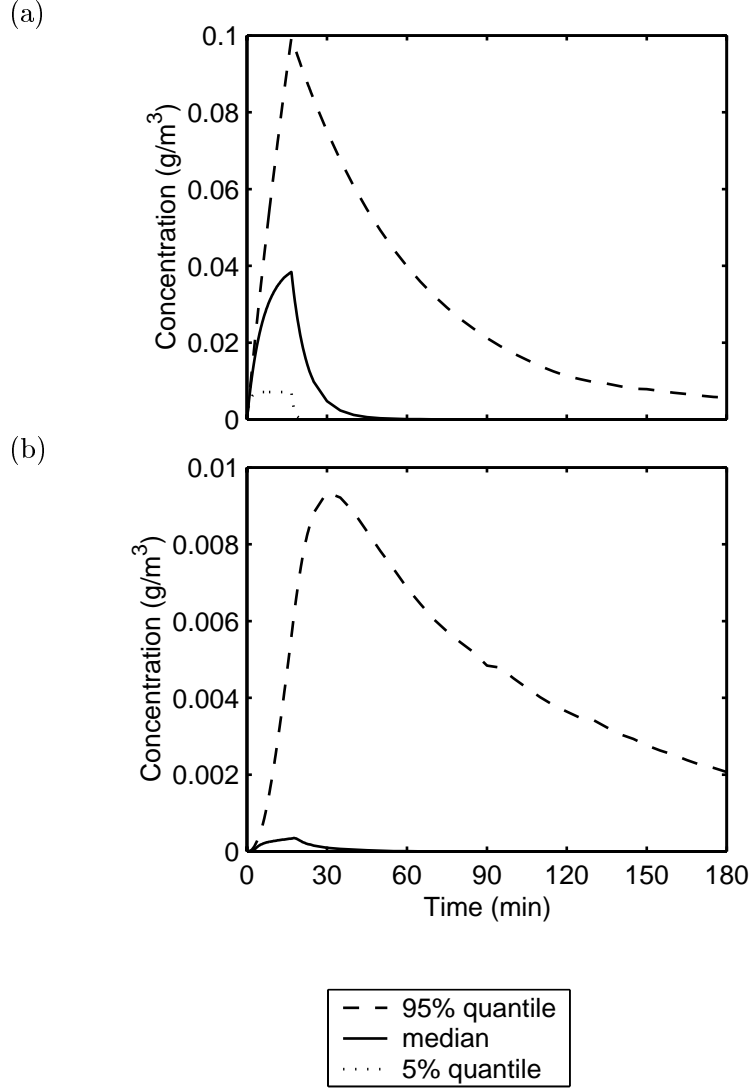

- - - 95% quantile
——— median
· · · · 5% quantile

Figure 3: Times-series concentration predictions for the central zones on the (a) first and (b) fifth floors from 2000 simulations. The pollutant is released in the central zone of the first floor for 16.7 minutes at 1 g/s. Note that the y-axis in (a) is a factor of 10 greater than in (b). The 5% quantile in (b) is at zero concentration and is not plotted. The net removal rate of pollutant, $\lambda = \Delta ln(C)/t$, for the 5%, median, and 95% quantiles are 0.85/min., 0.14/min., and 0.02/ min., respectively, on the first floor zone and the median and 95% quantiles are 0.16/min. and 0.01/min., respectively, on the fifth floor zone. The nominal time constant of air, $\tau = v/q$, for the 5%, median, and 95% quantiles are 47 min., 5.4 min., and 1 min., respectively, on the first floor zone and 49 min., 5.4 min., and 1.1 min., respectively, on the fifth floor zone.
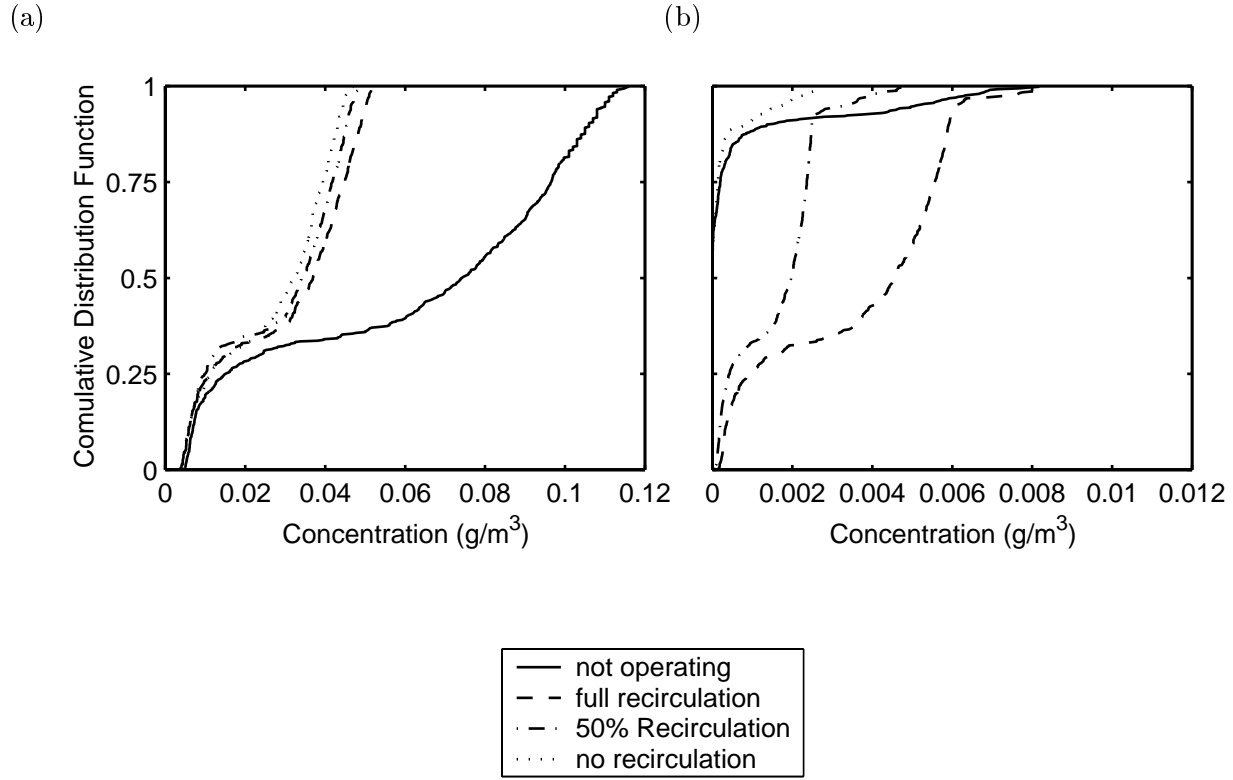
(a) (b)

Figure 4: Cumulative distribution functions for the predicted concentrations in the central zone of the (a) first and (b) fifth floors at time t=16.7 minutes for different HVAC conditions. The pollutant is released in the central zone of the first floor at 1 g/s for 16.7 minutes. Note that the x-axis in (a) is a factor of 10 greater than in (b).
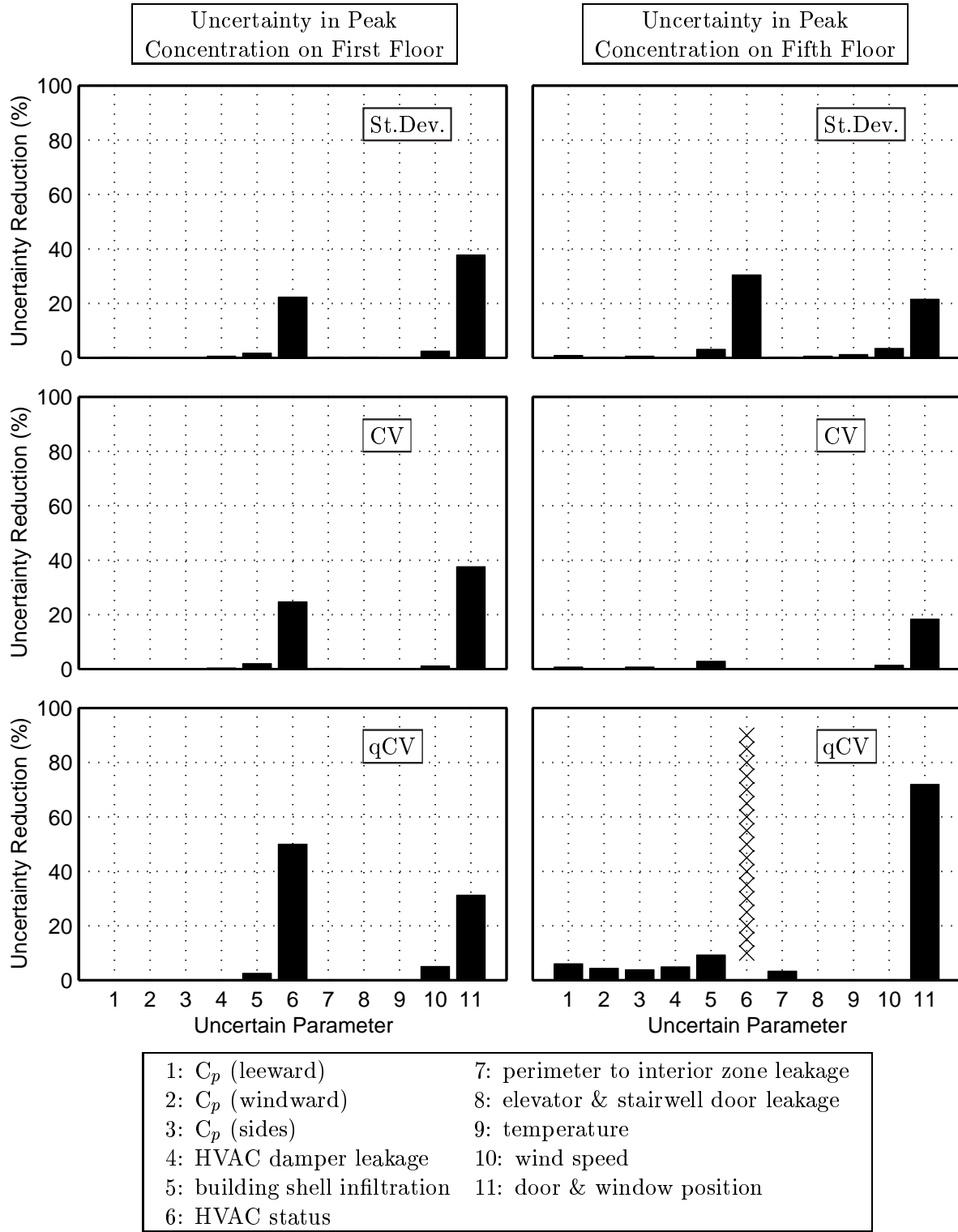
Figure 5: Reducing uncertainty in predictions of the peak concentration. The height of each bar refers to the reduction in end-point uncertainty from increased information about the parameter identified by numeric labels on the x-axis. Zero means uncertainty is not reduced and 100 percent means all of the uncertainty is removed. The fifth floor qCV estimate for HVAC operation is not calculated because the denominator (the median) was zero in one of the HVAC operating conditions (HVAC on with no recirculation).